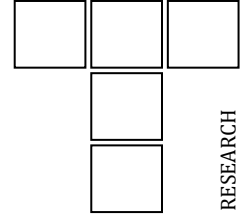




DOI: 10.24874/ti.1924.03.25.11

Tribology in Industry

www.tribology.rs



Investigating the Impact of Start-Stop Cycles on Gas Engine Oils Using a 4-Ball Tester

Rupesh Roshan^{a,*} , Siddhartha Sharma^b 

^aGreen Fuel and Lube Solutions, AR Design and Technology, Bangalore, Karnataka, 560067, India,

^bMechanical Department, National Institute of Technology Hamirpur, Himachal Pradesh, 177005, India.

Keywords:

Gas engine oil
Continuous run
Cold start
Start-stop operation
Friction
Wear
Additives

ABSTRACT

The increasing integration of renewable energy sources such as wind and solar has increased the need for modern power generation systems to operate with enhanced flexibility to manage variable electricity demands. However, frequent start-stop operations in these systems expose engine components and lubricants to severe thermal and mechanical stresses. To ensure long-term reliability, understanding the performance of gas engine oils under both steady and variable conditions is crucial. This study investigates the tribological characteristics of gas engine lubricants using a 4-ball tester to simulate realistic start-stop cycles. Friction coefficients and wear volumes were measured to evaluate oil performance. Results indicate that intermittent start-stop operation nearly doubled the friction coefficient to 0.075–0.11 compared with 0.04–0.055 during continuous running, particularly in transitional stages before complete oil film formation. Moreover, repeated start-stop cycles resulted in elevated wear rates, as used oil analysis revealed higher concentrations of wear metals, including iron, copper, and tin.

* Corresponding author:

Rupesh Roshan
E-mail: roshan@myardt.com

Received: 29 March 2025

Revised: 18 June 2025

Accepted: 16 November 2025



© 2026 Published by Faculty of Engineering

1. INTRODUCTION

Modern power generation systems must be flexible to accommodate fluctuating electricity demand and integrate intermittent energy sources like wind and solar, along with uncertainties such as faults. Traditionally, flexibility has been provided by conventional generation units that adjust output and start or shut down as needed [1]. However, this shift challenges existing plants not built for high variability, as frequent ramping and cycling increase equipment wear, maintenance costs, and

operational inefficiencies [2]. Modern plants, by contrast, demonstrate adaptability through the use of fuels such as natural gas, diesel, and biomass. Their modular designs allow rapid power adjustments, enabling operators to start, stop, or ramp engines efficiently. This flexibility is essential for grid stability, with gas engines offering rapid response compared to slower coal or nuclear plants [3,4].

Stationary gas engines are widely employed in distributed and small-scale power generation,

particularly in peaking plants where rapid start-up is essential to meet high electricity demand [5]. While reliant on a consistent natural gas supply and regular maintenance, they play a critical role in providing baseload and backup power, especially in regions emphasizing renewable energy integration and grid stability. Unlike conventional diesel or petrol engines, stationary gas engines undergo frequent start-stop cycles, subjecting components to higher mechanical stress [4–9]. Such cycling presents tribological challenges, as lubricants must withstand cold-start wear, temperature fluctuations, and viscosity variations. These stresses accelerate oil degradation, increasing maintenance needs and reducing engine longevity. Although advanced lubricants with specialized additives improve cold-start performance, wear resistance, and thermal stability, frequent cycling continues to shorten engine life and necessitate more frequent oil replacement [4,10].

Understanding the tribological behaviour of gas engine oils under both start-stop and continuous full-load conditions are critical for optimizing power generation performance [11]. Frequent start-stop cycles increase friction and wear due to insufficient lubrication during cold starts [12]. In gas-fired power plants, thickened oil during cold starts impedes circulation, accelerating wear on pistons, piston rings, and bearings. Short operating periods can also cause fuel dilution, moisture contamination, and oil nitration, further degrading oil quality [10]. Low oil levels, leaks, or mixing with fuel or coolant worsen friction and component wear, while

sludge and varnish build-up impairs lubrication [13,14]. Repeated start-stop cycles accelerate oil degradation, causing oxidation, viscosity changes, blocked passages, and increased wear, ultimately reducing engine efficiency, reliability, and lifespan [14–17].

This study investigated the tribological impact of start-stop cycles on gas engine oils, focusing on friction, wear, and lubricant degradation. Fresh oils were tested with the 4-ball tribometer to compare friction and wear behavior under short-duration start-stop cycles versus continuous operation. Additionally, oils collected from field gas engines with approximately 1,400 operating hours were analyzed to assess the effects of start-stop cycles on oil stability and performance. Both tribometer-tested and field-sourced oils were examined for physicochemical properties, additive degradation, and wear elements, providing insights into how frequent start-stop cycles affect friction, wear, and overall engine performance in stationary gas engines.

2. OIL SAMPLES

The study evaluated three commercially available gas engine oils: Mobil Pegasus 1005 (Oil1), Taurus GEO CH G240 (Oil2), and Sentron LD 8000 (Oil3), which are commonly used in natural gas engines. Engine oils from different manufacturers, even when sharing the same SAE viscosity grade, do not necessarily demonstrate identical lubricity performance in engines [18].

Table 1. Properties of the gas engine oils [17,18].

Lubricant - Type (SAE 40)	Oil1	Oil2	Oil3
Parameters (unit), Method	Mobil Pegasus 1005	Taurus GEO CH G240	Sentron LD 8000
KV @ 40 °C (cSt), ASTM D445	125	118	121
KV @ 100 °C (cSt), ASTM D445	13	13.8	13.3
TBN (mgKOH/g), ASTM D664	5	5.5	4.6
TAN (mgKOH/g), ASTM D2896	1.1	--	0.86
Flash point (°C), ASTM D93	247	268	277
Pour point (°C), ASTM D97	-15	-30	-27
Sulphated ash (wt.%), ASTM D874	0.5	0.49	0.52

The selected oil samples are mineral-based SAE 40 oils, as stationary gas engines typically operate under steady loads where oil degradation is primarily caused by

contamination rather than heat. Additionally, mineral-based gas engine oils provide sufficient oxidation stability, cost-effectiveness, and low-ash control, making semi-synthetic or synthetic

alternatives unnecessary and less compatible with OEM low-ash specifications. The chemical and physical properties of these oils are summarized in Table 1, offering a comprehensive comparison of their performance and suitability under various operating conditions [19,20].

3. TEST METHODOLOGY

3.1 Experimental setup

Various bench test rigs, such as reciprocating and unidirectional sliding setups, can be employed to assess oil performance under start-stop conditions. In this study, the commercially available 4-ball tester was chosen for its simplicity, precise control, reproducibility, and cost efficiency. This instrument effectively evaluates the friction and wear behaviour of lubricants under conditions representative of real engine environments [21]. The 4-ball tester was used to replicate boundary lubrication during start-stop cycles, simulating the high-pressure and low-speed conditions typical of gas engines [22,23].

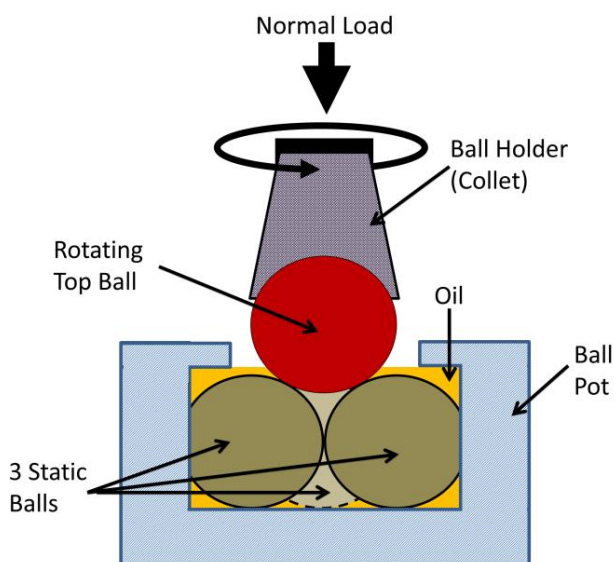


Fig. 1. Schematic diagram of the 4-ball apparatus.

The 4-ball tester (Ducom TR-30TM series) comprises an oil cup assembly, collet, and ball bearings, enabling accurate measurement of a lubricant's friction coefficient and wear performance. As shown in Figure 1, three stationary balls are positioned on a conical base, with a rotating ball placed on top under controlled

load conditions [24,25]. New balls were used for each test; all components were cleaned with acetone and thoroughly dried before use. The steel ball bearings were secured in the oil cup assembly using a torque wrench to prevent movement during testing [26]. The rotating ball simulated sliding motion under specific loads, speeds, and temperatures to generate friction and wear between contact surfaces. Following each test, the wear scars were examined to determine the lubricant's ability to reduce wear and form a protective film [18]. Wear scar diameters were measured using a high-resolution microscope to evaluate wear resistance [27,28].

3.2 Gas generator/engine

Key tribological parameters were derived through a theoretical analysis of data obtained from a Jenbacher 616 E gas generator/engine, as summarized in Table 2.

Table 2. Gas generator/engine data.

Engine Data	Values
Gas generator / Engine - make/ model	Jenbacher 616 E
Max. power rating, KW	approx. 2400
Number of cylinders	16
Bore (mm)	190
Stroke (mm)	220
Engine speed (rpm)	1500
Peak gas pressure (MPa)	22
Mean piston speed (m/s)	11
Cooling system return temperature (°C)	70
Cooling system supply temperature (°C)	90

3.3 Simulating gas engine conditions in a 4-ball tester

The gas engine primarily operates at a steady-state speed, with load variations driven by power demand and start-stop cycles. During start-up and shutdown, reduced oil pressure and temperature promote boundary lubrication, resulting in increased friction and wear on engine components. Birch [12] reported that frequent start-stop operation, typically involving 10-20-minute cycles, elevates mechanical stress, accelerates lubricant degradation, and increases friction during transitions from rest to motion. In

such conditions, inadequate oil warming intensifies wear and deteriorates the lubricant's chemical and physical properties [29]. Cold starts further exacerbate this effect, as high oil viscosity restricts circulation and raises friction until optimal viscosity is reached [1,30]. The 4-ball tester, commonly employed to assess lubricant tribological performance under controlled severe conditions, was used in this study. Continuous tests followed ASTM D4172, while modified start-stop tests simulated boundary conditions representative of piston ring-cylinder liner interactions.

Table 3. Gas engine simulated conditions in a 4-ball tester.

Operational Parameters	Jenbacher 616 E gas engine
Operating contact stress, GPa	2.7 (at top compression ring)
Sliding speed, m/s	0.38 (at 1° crank angle near dead centre)
Oil temperature, °C	80 (oil temperature after 10 min of start)
Start-stop duration, min	10-15 (Cold start to full load)

Key engine parameters, including sliding speed, contact stress, and oil temperature, are essential for reproducing realistic operating conditions in tribological evaluations. Table 3 outlines the severe operating conditions of the Jenbacher 616 E gas engine and the corresponding parameters replicated in the 4-ball tester. The selected pressure, temperature, and speed values reflect boundary lubrication conditions typically occurring near the top and bottom dead centres (TDC and BDC). At approximately 1° crank angle, the top compression ring experiences a sliding velocity of 0.38 m/s and a contact stress of 2.7 GPa. The oil temperature rises to 80 °C within 10–15 minutes, simulating the transition from cold start to full-load operation. In the 4-ball tester, comparable conditions were achieved with a contact stress of 2.4 GPa, a sliding speed of 0.34 m/s, and a temperature of 75 °C. Here, the contact pressure between the balls was calculated using equations 1 and 2.

$$P_{max} = \frac{3F}{2\pi a^2} \quad (1)$$

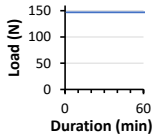
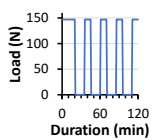
$$a = \sqrt[3]{\frac{3F \left(\frac{1-\nu_1^2}{E_1} + \frac{1-\nu_2^2}{E_2} \right)}{4 \left(\frac{1}{R_1} + \frac{1}{R_2} \right)}} \quad (2)$$

Where, ν_1 and ν_2 denote the Poisson's ratios of the two ball materials (0.3), while E_1 and E_2 represent their moduli of elasticity (210 GPa). R_1 and R_2 correspond to the radii of curvature of the balls (12.7 mm). P_{max} refers to the maximum contact pressure between the balls, defined as the force per unit area at the point of contact. This pressure is determined by the applied load, the material properties, and the geometric configuration of the balls.

3.4 Methods for continuous and start-stop testing

The test conditions and procedures used to assess the effects of continuous operation and intermittent on/off load cycles in the 4-ball tester are summarized in Table 4. Continuous tests were performed under a constant load of 147N (2.5 GPa), at 1200 rpm, and a temperature of 75 °C for a duration of 60 minutes.

Table 4. Continuous run and simulated start-stop test.

Test Method	Continuous Run (ASTM D4172)	Simulated Start-Stop Test
Start-Stop cycle	none	Start with a 20-minute initial run, and then 10-minute run after each 15-minute rest period. Continue this cycle until a total of 60 minutes run is reached
Load (N) / Loading Cycle	147	147 (load during running phase) and no load during stop condition
		
Speed (rpm)	1200	1200
Temperature (°C)	75±1	75±1
Oil quantity (ml)	~15	~15
Total test duration (min)	60	120
Run duration (min)	60	60

The start-stop test was designed to assess oil performance under rapid changes in operational conditions, particularly from cold starts to high-speed operation. Its purpose was to evaluate the oils' effectiveness in reducing friction and providing wear protection, using run durations comparable to continuous tests. Key parameters, including start/stop times, rest intervals, and cycle repetitions, were maintained consistently. The procedure involved a 60-minute active run, structured to replicate the fast transitions typical in gas engines. Each test began with a 20-minute run at 1200 rpm under a 40 kg load, followed by 10 minutes of operation after each 15-minute rest period, with friction and temperature carefully monitored. The start-stop cycles, executed by initiating and halting rotation of the top ball, were repeated four times over a total duration of 120 minutes to evaluate the oil's ability to sustain a stable lubrication film and prevent increased wear.

4. RESULTS

The friction and wear performance of fresh gas engine oils (Oil1, Oil2, and Oil3) was evaluated under continuous and start-stop conditions according to the procedures in Table 4. Each test was repeated three times to ensure consistent and reliable results. For Oil1, Figure 2 shows the coefficient of friction (COF) under both continuous and simulated start-stop conditions, with minimal variation in instantaneous COF across repetitions, demonstrating reproducibility and statistical confidence.

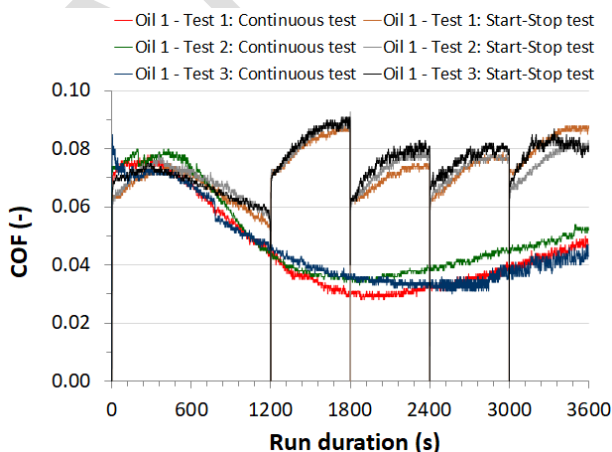


Fig. 2. COF for Oil1 during repeated tests under continuous and start-stop operation.

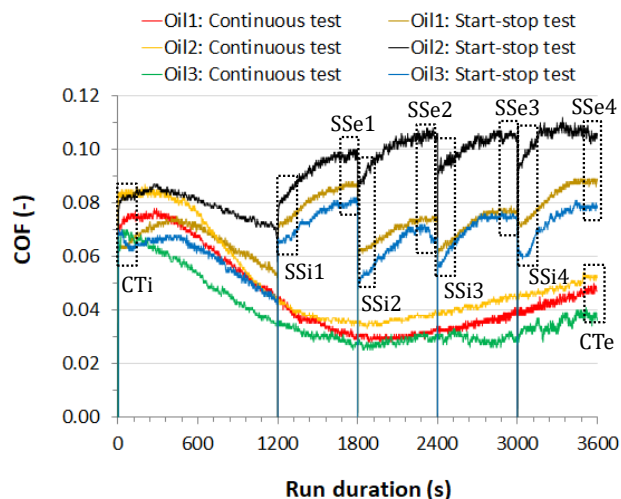


Fig. 3. Comparison of the COF for continuous and start-stop runs for the oils.

Fig 3 illustrates the COF for the engine oils, Oil1, Oil2, and Oil3, under continuous and simulated start-stop conditions. Variations in COF reflect oil's effective lubrication under changing operating conditions. Initially, all oils showed similar friction trends. During continuous operation, the COF decreases and stabilizes between 0.04–0.055, whereas it rises to 0.075–0.11 during start-stop cycles. Temperature fluctuations of ± 4 °C during start-stop operation affected COF stability, while interruptions in the lubrication film further elevated COF, highlighting the oils' performance under dynamic conditions [31].

5. DISCUSSIONS

5.1 Effect of start-stop cycle on friction

Fig 4 presents the average initial and end COF for oils Oil1, Oil2, and Oil3, comparing their behaviour under continuous operation and start-stop cycle conditions. The initial COF for oils was determined by averaging the first and last two minutes of instantaneous COF data from each test, including start-up periods following rest intervals, as illustrated in Figure 3. The intervals labelled 'CTi' and 'CTe' represent the periods used to compute the mean COF at the start and end of the continuous test, while 'SSi' and 'SSe' correspond to equivalent durations for the start-stop cycle.

The results indicate that the start-stop sequence caused a slight increase in the initial

COF (approximately +0.01), with Oil3 exhibiting the lowest and Oil2 the highest initial values. During continuous operation, all oils showed a reduction in final COF to the range of 0.04–0.055, while under start-stop conditions, the COF nearly doubled to 0.075–0.11. Among the samples, Oil2 displayed the most pronounced increase, reaching a COF of 0.09. Repeated interruptions during start-stop cycles resulted in higher friction levels than during steady-state operation, along with greater variability and notable temperature oscillations. Similar trends were reported by Stephen et al. [32] and Shafi and Charoo [33], who attributed increased COF to temporary breakdowns of the lubricant film during intermittent motion. The elevated COF observed in start-stop cycles can also be linked to abrasive wear, as extreme-pressure and anti-wear additives require approximately 400 seconds to form a stable protective tribofilm, as noted by Chen et al. [34].

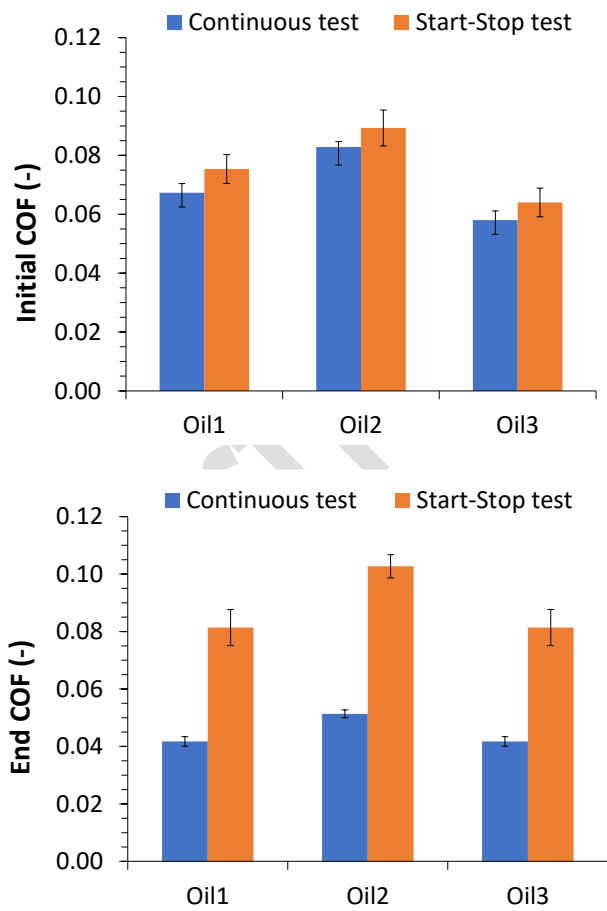


Fig. 4. Initial and end COF under continuous and simulated start-stop operating conditions.

5.2 Effect of start-stop cycle on wear

Fig 5 presents the wear scar diameter (WSD) and wear volume obtained from continuous and simulated start-stop tests, used to compare the anti-wear performance of Oil1, Oil2, and Oil3. Post-test wear on the three stationary balls was measured using an optical 3D profilometer. Both WSD and wear volume were analyzed, as the latter provides a more comprehensive assessment of wear severity. In contrast to WSD, wear volume accounts for material displacement, transfer, and the irregular geometry of wear scars produced by sliding contact between the rotating and stationary balls, thus offering a more accurate representation of surface degradation [35].

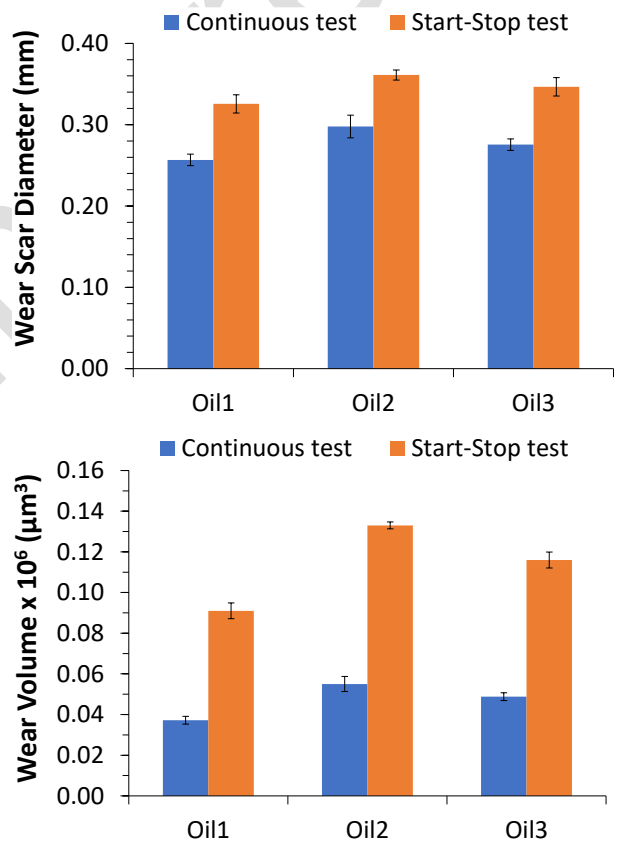


Fig. 5. Wear scar diameter and wear volume under steady and simulated start-stop operating conditions.

Low wear volumes and scars indicate superior lubrication and reduced metal-to-metal interaction. The results show that both wear volume and WSD were consistently higher during start-stop tests than in continuous runs. The increased wear observed under start-stop conditions is attributed to greater asperity contact, elevated localized stresses, and surface

alterations following each rest period. In contrast, continuous operation produced lower WSD and wear volume values, reflecting more stable lubrication. Among the tested oils, Oil2 and Oil3 exhibited the poorest performance, showing the highest wear volumes under both test conditions, confirming its weaker anti-wear capability compared to Oil1.

5.3 Effect of start-stop cycle on oil deterioration

During real-world operation, gas engine oils undergo gradual degradation resulting from physical and chemical aging processes driven by stress, oxidation, and contamination. This deterioration is further accelerated by combustion residues, temperature variations, and start-stop cycles [36]. To evaluate their impact on lubrication performance, fresh, used, and test-aged oils were analyzed for physical and chemical properties. Oils obtained after 1400 hours of operation from a Jenbacher 616 E gas engine (Oil1g, Oil2g, Oil3g; see Table 5) and after start-stop tests in a 4-ball tester (Oil1b, Oil2b, Oil3b) were examined to correlate friction and wear behaviour with the oil condition. Engine oil samples were collected from the sump before filtration using a clean device under normal operating temperature and load to ensure sample integrity [21]. Oils subjected to continuous 4-ball tests were excluded, as their properties remained similar to fresh oils.

Table 5. Used oil samples from Jenbacher 616 E gas generator/engine.

Lubricant Type (SAE 40)	Oil1g (Mobil Pegasus 1005)	Oil2g (Taurus GEO CH G240)	Oil3g (Sentron LD 8000)
Ambient temperature (°C)	9		
Run hours after overhaul, (hrs)	1396	1407	1405

Table 6 compares the physicochemical properties of fresh oils, samples obtained after the 4-ball start-stop tests, and those collected from the Jenbacher 616 E gas engine. Post-test oils (Oil1b–3b) displayed slight decreases in kinematic viscosity and flash point, accompanied by minor shifts in TAN and TBN values. In contrast, oils retrieved from engine

operation (Oil1g–3g) exhibited more pronounced viscosity loss and acidity increase, particularly in Oil2g, indicating oxidative degradation and depletion of additives under real operating conditions. These variations correspond with the elevated wear and friction levels observed in the 4-ball tests, highlighting that oils with greater viscosity stability and oxidation resistance, such as Oil1, deliver improved tribological behaviour.

Table 6. A comparison of physicochemical properties of the fresh and used oils.

Oils/ ASTM Method/ Unit	KV @ 40 °C (D446)	KV @ 100 °C (D446)	Flash Point (D94)	Pour Point (D98)	TAN (D665)	TBN (D2897)
	cSt		°C		mgKOH/gm	
Fresh oil samples						
Oil1	126	14.0	247	-21	1.05	4.9
Oil2	122	13.5	240	-21	0.70	5.1
Oil3	119	13.6	266	-27	0.66	4.6
Sample collected post 4-ball start-stop test						
Oil1b	124	14.0	246	-21	1.03	4.2
Oil2b	116	13.1	232	-21	1.13	4.8
Oil3b	118	13.4	261	-27	0.68	4.4
Sample collected from the Jenbacher 616 E gas engine						
Oil1g	117	13.4	231	-18	1.20	3.9
Oil2g	115	13.2	220	-18	1.41	4.1
Oil3g	114	13.1	234	-24	0.74	4.1
Limit	-20 / +30%		< 180	vary	+ 2.5	50% Drop

The friction and wear results presented in Figures 3–5 further support the findings summarized in Table 6. Oil1 exhibited minimal wear and low friction coefficients, which can be attributed to its high viscosity (124 cSt at 40 °C). Oil2 showed the highest wear, corresponding to its lower viscosity (116 cSt), while Oil3 displayed intermediate behaviour, consistent with its moderate viscosity (118 cSt) and strong oxidation stability (Δ TAN < 1.0 mgKOH/g).

Table 7 presents the concentrations of additive elements in fresh oils (Oil1–Oil3), in post-4-ball start-stop test samples (Oil1b–Oil3b), and in oils obtained from the Jenbacher 616 E engine (Oil1g–Oil3g), as analyzed using the ASTM D5185 method. Among the tested

samples, Oil1 demonstrated the lowest wear and friction, reflecting efficient anti-wear and friction-reducing capabilities attributed to its high calcium (1630 ppm) and boron (99.6 ppm) contents. In contrast, Oil2 exhibited the highest wear (0.36 mm) and friction ($\mu = 0.103$), which corresponded to minimal boron (0.7 ppm) and moderate depletion of calcium (ΔCa : 32 ppm), zinc (ΔZn : 31 ppm), and phosphorus (ΔP : 27 ppm). Oil3b showed intermediate tribological behavior, with minimal reductions in calcium (ΔCa : 15 ppm), zinc (ΔZn : 3 ppm), and phosphorus (ΔP : 4 ppm), combined with elevated magnesium (10.1 ppm), providing balanced anti-wear protection. During engine operation, all samples exhibited further zinc and phosphorus depletion, confirming ZDDP consumption. Oil1g maintained higher additive concentrations and better performance, while Oil2g experienced the greatest reductions (ΔZn : 80 ppm; ΔP : 47 ppm). Overall, oils with stable anti-wear (Zn, P) and detergent/dispersant (Ca, B, Mg) additives, particularly Oil1, demonstrated superior friction and wear performance, consistent with the findings of Thapliyal and Thakre [37] and Konkol et al. [38].

Table 7. A comparison of additive elements in the fresh and used oils.

Oils	Additive elements, ASTM D5185 (ppm)					
	B	Ca	Mg	Mo	P	Zn
Fresh oil samples						
Oil1	99.6	1630	8.3	<.01	345	380
Oil2	0.7	1535	4.7	<.01	418	360
Oil3	1.6	1497	10.1	<.01	332	351
Sample collected post 4-ball start-stop test						
Oil1b	101.8	1590	7.6	<.01	341	374
Oil2b	1.1	1503	4.9	<.01	387	333
Oil3b	1.4	1482	9.8	<.01	329	347
Sample collected from the Jenbacher 616 E gas engine						
Oil1g	112.7	1547	6.4	<.01	333	356
Oil2g	2.2	1476	8.1	<.01	340	280
Oil3g	2.3	1445	9.2	<.01	302	345

Table 8 compares wear element concentrations in fresh oils, oils after the 4-ball start-stop test, and oils from a Jenbacher 616 E gas engine. Fresh oils exhibit negligible levels of wear

elements (<0.01 ppm), confirming the absence of initial wear or contamination. Following the 4-ball test, moderate increases in Fe, Cu, Al, and Sn indicate slight wear under controlled conditions. Oils used in the engine show higher concentrations of wear elements, reflecting considerable wear during operation, yet remaining within acceptable limits. The correlation between wear element concentrations and tribological performance indicates that Oil1b contained modest Fe, Cu, and Al levels, corresponding to low wear (WSD: 0.32 mm) and moderate friction (0.075–0.081). Oil2b exhibited higher Fe (0.8 ppm) and Sn (0.6 ppm), consistent with greater wear (WSD: 0.36 mm) and friction (0.075–0.11), while Oil3b showed intermediate values. Engine oil samples supported these patterns, with Oil2g exhibiting the highest metal concentrations and Oil3g the lowest, confirming that operational stress accelerates lubricant degradation, in agreement with previous findings [39].

Table 8. A comparison of wear elements in the fresh and used oils.

Oils	Wear elements, ASTM D5185 (ppm)						
	Fe	Cu	Al	Sb	Ni	Ag	Sn
Fresh oil samples							
Oil1	<.01						
Oil2	<.01						
Oil3	<.01						
Sample collected post 4-ball start-stop test							
Oil1b	0.5	3.1	1.8	0.6	<.01	0.6	0.7
Oil2b	0.8	1.2	0.4	0.9	0.2	0.3	0.6
Oil3b	0.7	0.8	1.3	0.8	<.01	0.4	<.01
Sample collected from the Jenbacher 616 E gas engine							
Oil1g	6.1	4.0	4.0	0.8	0.7	1.4	1.2
Oil2g	9.8	11	5.5	1.2	0.5	1.6	3.3
Oil3g	3.9	3.2	2.2	0.9	0.2	1.5	0.8
Limit	30	15	10	10	10	10	10

6. CONCLUSION

The study examines the effects of start-stop cycles on the friction, wear, and degradation of engine oils. Simulated start-stop conditions caused higher friction and wear due to lubrication disruption and temperature variation during start-up. Compared with continuous operation, where friction remained

low and stable, start-stop cycles produced more variable and nearly doubled end coefficients of friction (COF). Initial COF values were similar across tests, with Oil3 showing the lowest and Oil2 the highest. Wear assessments revealed larger wear scar diameters and volumes under intermittent motion, indicating intensified asperity contact and localized stress. Oil1 demonstrated the best anti-wear performance, while Oil2 showed the highest wear. Post 4-ball and 1400-hour engine tests indicated viscosity reduction, additive depletion, and increased acidity, especially in Oil2g, confirming oxidative degradation. Retention of Zn, P, Ca, B, and Mg correlated with lower friction and wear. Accumulation of Fe, Cu, Al, and Sn confirmed progressive wear, emphasizing that additive stability is essential to withstand start-stop-induced lubricant deterioration. Further studies under varying conditions can be performed to generalize these findings.

Acknowledgment

The authors would like to thank SembCorp Industries for providing the gas engine oil samples and extend their gratitude to the university laboratory for their assistance with the tribology and oil analysis tests.

Declaration

The authors declare no competing financial or personal interests influencing this work reported in this paper.

REFERENCES

- [1] A. Alahäivälä, J. Kiviluoma, J. Leino, and M. Lehtonen, "System-Level Value of a Gas Engine Power Plant in Electricity and Reserve Production," *Energies*, vol. 10, no. 7, pp. 983, Jul. 2017, doi: 10.3390/en10070983.
- [2] M. L. Kubik, P. J. Coker, and C. Hunt, "The Role of Conventional Generation in Managing Variability," *Energy Policy*, vol. 50, pp. 253–261, Aug. 2012, doi: 10.1016/j.enpol.2012.07.010.
- [3] H. Al-Rawashdeh, O. A. Al-Khashman, J. T. Al Bdour, M. R. Gomaa, H. Rezk, A. Marashli, L. M. Arrfou, and M. Louzazni, "Performance Analysis of a Hybrid Renewable-Energy System For Green Buildings to Improve Efficiency and Reduce GHG Emissions With Multiple Scenarios," *Sustainability*, vol. 15, no. 9, pp. 7529, May 2023, doi: 10.3390/su15097529.
- [4] F. Kiefer, "Efficiency Challenges For Gas Engines," Infineum Insight, Accessed Feb. 12, 2025 [Online]. Available: <https://www.infineuminsight.com/en-gb/articles/efficiency-challenges-for-gas-engines>
- [5] C. Guido, P. Napolitano, D. Di Domenico, D. Di Maio, C. Beatrice, B. Griffaton, and N. Obrecht, "Exploiting Lubricant Formulation to Reduce Particle Emissions From Gas Powered Engines," *Energies*, vol. 17, no. 15, pp. 3781, Jul. 2024, doi: 10.3390/en17153781.
- [6] M. Nielsen, J. B. Illerup, and K. Birr-Petersen, "Revised Emission Factors for Gas Engines Including Start/Stop Emissions", NERI Technical Report, National Environmental Research Institute, University of Aarhus, 2008. [Online]. Available: <http://www.dmu.dk/Pub/FR672.pdf>
- [7] R. Scott, "Stationary Natural Gas Engine Lubrication," Machinery Lubrication, Accessed: May 12, 2025. [Online]. Available: <https://www.machinerylubrication.com/Read/663/natural-gas-engine>
- [8] C. Thirion and J. W. Steyn, "Natural Gas for Power Generation", Owner Team Consultation. Accessed: Apr. 30, 2025. [Online]. Available: <https://www.ownerteamconsult.com/natural-gas-for-power-generation>
- [9] G. Pirker and A. Wimmer, "Sustainable Power Generation with Large Gas Engines," *Energy Conversion and Management*, vol. 149, pp. 1048–1065, Jun. 2017, doi: 10.1016/j.enconman.2017.06.023.
- [10] N. Dayanand, J. D. Palazzotto, and A. T. Beckman, "Effect of Stationary Natural Gas Engine Oils on Fuel Economy," *Proceedings of the ASME Internal Combustion Engine Division Spring Technical Conference*, pp. 925–932, Jul. 2013, doi: 10.1115/ICES2012-81052.
- [11] T. K. Jensen, J. De Wit, S. D. Andersen, H. Frederiksen, and M. Nielsen, "The Influence of Engine Start and Stop on Total Emission from Natural Gas Fired CHP Engines," in *International Gas Union Research Conference (IGRC 2008), Danish Gas Technology Centre and National Environmental Research Institute (DMU)*, 2008.
- [12] S. Birch, "Racing to Solve the Lubrication Challenges of Stop/Start-Equipped Engines," International, Mobility Engineering, Accessed: Nov. 18, 2025. [Online]. Available: <https://www.mobilityengineeringtech.com/component/content/article/41919-sae-ma-01108>

- [13] M. Karrouchi, M. Rhiat, I. Nasri, I. Atmane, K. Hirech, A. Messaoudi, M. Melhaoui, and K. Kassmi, "Practical Investigation and Evaluation of the Start/Stop System's Impact on the Engine's Fuel Use, Noise Output, and Pollutant Emissions," *e-Prime - Advances in Electrical Engineering Electronics and Energy*, vol. 6, pp. 925-932, Oct. 2023, doi: 10.1016/j.prime.2023.100310.
- [14] Infineum Insight, "Gas Engine Formulation Challenges," Accessed: May 31, 2024, [Online]. <https://www.infineuminsight.com/en-gb/articles/gas-engine-formulation-challenges>
- [15] T. Schasfoort and C. Buhler, "Gas Engine Reliability: Understanding Engine Oil Consumption," Petro-Canada Lubricants, Accessed: Sept. 12, 2024. [Online]. Available: <https://www.powermag.com/gas-engine-reliability-understanding-engine-oil-consumption/>
- [16] D. Bražinskienė, A. Ručinskienė, and S. Asadauskas, "Miniaturization of Lubricant Degradation Testing for Natural Gas Engines," in *Proceedings 8th International Conference BALTRIB'2015*, Nov. 2015, doi: 10.15544/baltrib.2015.01.
- [17] S. Rațiu, A. Josan, V. Alexa, V. G. Cioată, and I. Kiss, "Impact of Contaminants on Engine Oil: A Review," *Journal of Physics Conference Series*, vol. 1781, no. 1, pp. 012051, Feb. 2021, doi: 10.1088/1742-6596/1781/1/012051.
- [18] A. N. Farhanah and M. Z. Bahak, "Engine Oil Wear Resistance," *Jurnal Tribologi*, vol. 4, pp. 10-20, Mar. 2015.
- [19] J. Čapek, "Engine Oil Charges For Stationary Gas TEDOM Engines," Yanmar Group, Regulation 61-0-0281.1, Dec. 6, 2006. [Online]. Available: https://www.tedom.com/wpcontent/uploads/2019/10/61-0-0281_1-Engine-oil-charges-for-stationary-gas-TEDOM-engines-11.pdf
- [20] L. Leugner, "Natural Gas Engine Lubrication and Oil Analysis," Maintenance Technology International, Inc., Machinery Lubrication, Accessed: Jan. 31, 2025. [Online]. Available: <https://www.machinerylubrication.com/Read/524/natural-gas-engine-oil-analysis>
- [21] R. S. Gates and S. M. Hsu, "Four-Ball Wear Test For Engine Oil Evaluation," *National Bureau Standard (U.S.), Spec. Publ.; (United States)*, vol. 584, no. 1, pp. 60-78, Nov. 1980.
- [22] V. Zin, F. Agresti, S. Barison, L. Colla, A. Gondolini, and M. Fabrizio, "The Synthesis and Effect of Copper Nanoparticles on The Tribological Properties of Lubricant Oils," *IEEE Transactions on Nanotechnology*, vol. 12, no. 5, pp. 751-759, Jul. 2013, doi: 10.1109/tnano.2013.2273566.
- [23] F. G. Rounds, "Soot From Used Diesel Engine Oils - Their Effects on Wear as Measured in 4-Ball Wear Tests," *SAE Technical Papers on CD-ROM/SAE Technical Paper Series*, vol. 1, Feb. 1981, doi: 10.4271/810499.
- [24] E. Hu, X. Hu, T. Liu, L. Fang, K. D. Dearn, and H. Xu, "The Role of Soot Particles in The Tribological Behaviour of Engine Lubricating Oils," *Wear*, vol. 304, no. 1-2, pp. 152-161, May 2013, doi: 10.1016/j.wear.2013.05.002.
- [25] A. Kumar, R. Chaudhary, and R. C. Singh, "Tribological Performance of Various Blends of Commercial SAE 40 Oil and Novel Apricot Oil-Based Bio-Lubricant Using a Four-Ball Tester Tribometer," *International Journal of Materials and Product Technology*, vol. 67, no. 2, pp. 166-177, Jan. 2023, doi: 10.1504/ijmpt.2023.133049.
- [26] G. Yadav, S. Tiwari, and M. L. Jain, "Tribological Analysis of Extreme Pressure and Anti-Wear Properties of Engine Lubricating Oil Using Four Ball Tester," *Materials Today Proceedings*, vol. 5, no. 1, pp. 248-253, Jan. 2018, doi: 10.1016/j.matpr.2017.11.079.
- [27] M. J. Valdes, J. G. A. Marín, M. A. Rodriguez-Cabal, and J. D. Betancur, "Tribometry: How is Friction Research Quantified? A Review," *International Journal of Engineering Research and Technology*, vol. 13, no. 10, pp. 2596, Oct. 2020, doi: 10.37624/IJERT/13.10.2020.2596-2610.
- [28] T. M. Al-Quraan, F. Alfaqs, J. Haddad, V. Vojtov, A. Voitov, A. Kravtsov, O. Miroshnyk, and A. Kondratiev, "A Methodological Approach to Assessing the Tribological Properties of Lubricants Using a Four-Ball Tribometer," *Lubricants*, vol. 11, no. 11, pp. 457, Oct. 2023, doi: 10.3390/lubricants11110457.
- [29] T. Bartels, "Mechanical-Dynamic Test Methods for Lubricants," in *Lubricants and Lubrication*, edition, T. Mang and W. Dresel, Eds. Weinheim, Germany, Dec. 2006, pp. 736-756.
- [30] F. König, C. Sous, and G. Jacobs, "Numerical Prediction of the Frictional Losses in Sliding Bearings during Start-Stop Operation," *Friction*, vol. 9, no. 3, pp. 583-597, Dec. 2020, doi: 10.1007/s40544-020-0417-9.
- [31] K. Sornek, M. Homa, F. M. Frigera-Iliasa, M. Frigera-Iliasa, M. Jankowski, K. Papis-Frączek, J. Katerla, and J. Janus, K. Sornek et al., "Power-To-Heat and Seasonal Thermal Energy Storage: Pathways Toward a Low-Carbon Future For District Heating," *Energies*, vol. 18, no. 21, pp. 5577, October 2025, doi: 10.3390/en18215577.
- [32] S. Stephan, S. Schmitt, H. Hasse, and H. M. Urbassek, "Molecular Dynamics Simulation of The Stribeck Curve: Boundary Lubrication,

- Mixed Lubrication, and Hydrodynamic Lubrication on the Atomistic Level,” *Friction*, vol. 11, no. 12, pp. 2342–2366, Jul. 2023, doi: 10.1007/s40544-023-0745-y.
- [33] W. K. Shafi and Charoo, “Antiwear and Extreme Pressure Properties of Hazelnut Oil Blended with ZDDP,” *Industrial Lubrication and Tribology*, vol. 73, no. 2, pp. 297–307, Nov. 2020, doi: 10.1108/ilt-06-2020-0217.
- [34] S. Chen, J. Cai, G. Xiang, J. Zhang, Z. Liu, and M. Fillon, “Tribo-Dynamic-Wear Coupling Analysis For Water-Lubricated Bearings With Journal Surface Imperfection Under Repeated Start-Stop Cycles,” *Tribology International*, vol. 200, pp. 110093, Aug. 2024, doi: 10.1016/j.triboint.2024.110093.
- [35] A. H. Battez, A. T. Pérez, G. García-Atanje, J. L. Viesca, R. G. Rodriguez and M. Hadfield, “Advantages of Using Optical Profilometry in the ASTM D4172 Standard,” in *Proceeding of STLE Annual Meeting and Exhibition*, Oct. 2010.
- [36] M. J. Schmeida, “Mid-Sized New Generation: Reciprocating Internal Combustion Engines or Combustion Turbine?,” in *Power-Gen 2017 Conference*, pp. 1–13, Oct. 2017.
- [37] P. Thapliyal and G. D. Thakre, “Correlation Study of Physicochemical, Rheological, and Tribological Parameters of Engine Oils,” *Advances in Tribology*, vol. 2017, pp. 1–12, Jan. 2017, doi: 10.1155/2017/1257607.
- [38] I. Konkol, J. Cebula, L. Świerczek, J. Sopa, J. Sopa, and A. Cenian, “Characterization of Deposits Formed in Gas Engines Fuelled by Coal Mine Methane,” *Materials*, vol. 16, no. 6, pp. 2517, Mar. 2023, doi: 10.3390/ma16062517.
- [39] M. M. Kallas, M. S. A. Sabek, and Y. Saoud, “Experimental Comparison of the Effect of Using Synthetic, Semi-Synthetic, And Mineral Engine Oil On Gasoline Engine Parts,” *Advances in Tribology*, vol. 2024, pp. 1–12, Apr. 2024, doi: 10.1155/2024/5997292.

NOMENCLATURE

Symbol	Description
Ag	silver
Al	aluminium
ASTM	American Society for Testing and Materials
B	boron
BDC	bottom dead centre
°C	degree Celsius
Ca	calcium
COF	coefficient of friction
CT	continuous test
Cu	copper
E ₁ , E ₂	Elastic Modulus (Material 1 and 2)
Fe	iron
GPa	gigapascal
KV	kinematic viscosity
m/s	meter per second
Mg	magnesium
Mo	molybdenum
MPa	megapascal
N	newton
Ni	nickel
P	phosphorus
P _{max}	maximum contact pressure
R ₁ , R ₂	radii of curvature (body 1 and 2)
Sb	antimony
Sn	tin
SS	start-stop